Supplement of Weather Clim. Dynam., 4, 567–589, 2023
https://doi.org/10.5194/wcd-4-567-2023-supplement

Supplement of

The relationship between extra-tropical cyclone intensity and precipitation in idealised current and future climates

Victoria A. Sinclair and Jennifer L. Catto

Correspondence to: Victoria A. Sinclair (victoria.sinclair@helsinki.fi)

S1 Sensitivity of the clusters to different radii

The input to the k-means clustering scheme was the precipitation within a radius of 12 degrees of the cyclone centre. The radius of 12 degrees was selected based on previous studies, however, here we assess whether the spatial patterns of precipitation in the resulting clusters are sensitive to the selected radius. To do this, the clustering was repeated but with various different radii: 4.5, 8, 12 and 18 degrees. The results are shown in Figure S1. Overall, the results are not sensitive to the choice of radius. The exception is when a small radius (4.5 degrees) was used and in that case the "centre ETC" (Fig. S1a) has weaker precipitation over a smaller area compared to when larger radii are used. Furthermore, the "warm front" ETC (Fig. S1b) has heavier precipitation associated with it then when larger radii are used.

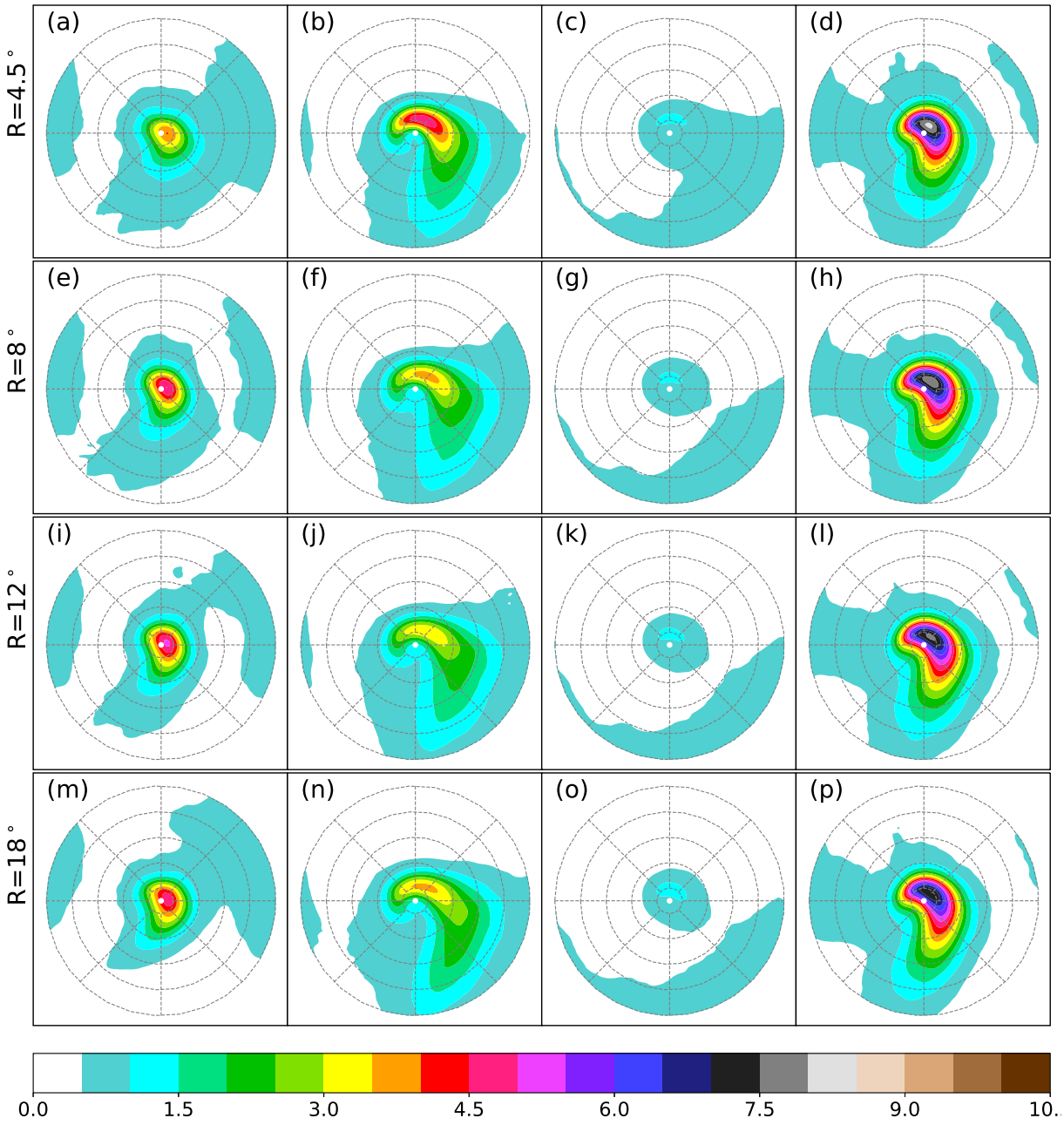

Figure S1: Cluster mean total precipitation (mm / 6 hr) 12 hours before the time of maximum vorticity for the control simulation. Clusters have been created with using different radii of the considered precipitation. Panels a-d show the cluster mean total precipitation when only precipitation within a radius of 4.5 degrees is considered, panels e-h for a radius of 8 degrees, panels i-l for a radius of 12 degrees and panels m-p for a radius of 18 degrees.

S2 Number of Clusters

Figure S2 shows the silhouette score for all three experiments as a function of cluster number. Large positive values mean that on average ETCs are very similar to the mean of the cluster they belong to and also very different from the means of the clusters that they do not belong to. Small or negative values (the silhoutte score ranges from 1 to -1) suggests poor or mis-classification. Therefore, the number of clusters is chosen based primarily on where the silhouette score is a localised maximum but also at a practical and manageable number of clusters.

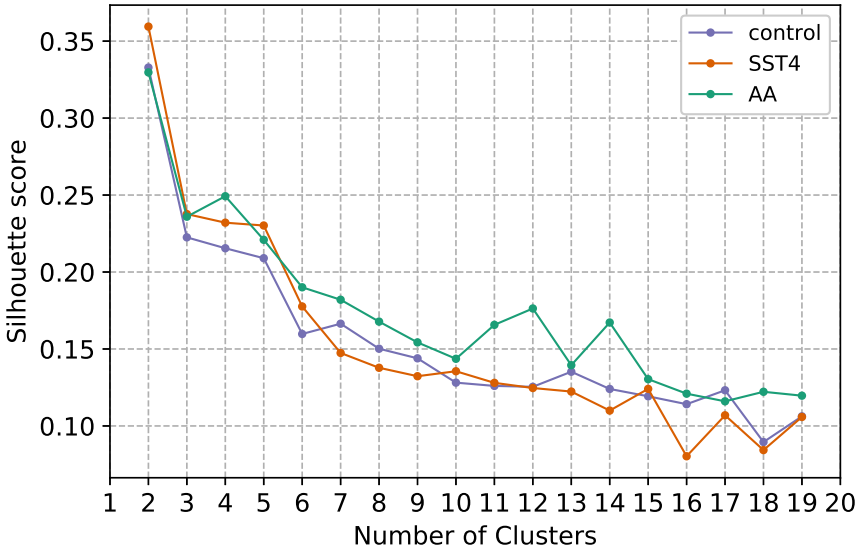

Figure S2: Silhouette score for different number of clusters for each experiment.

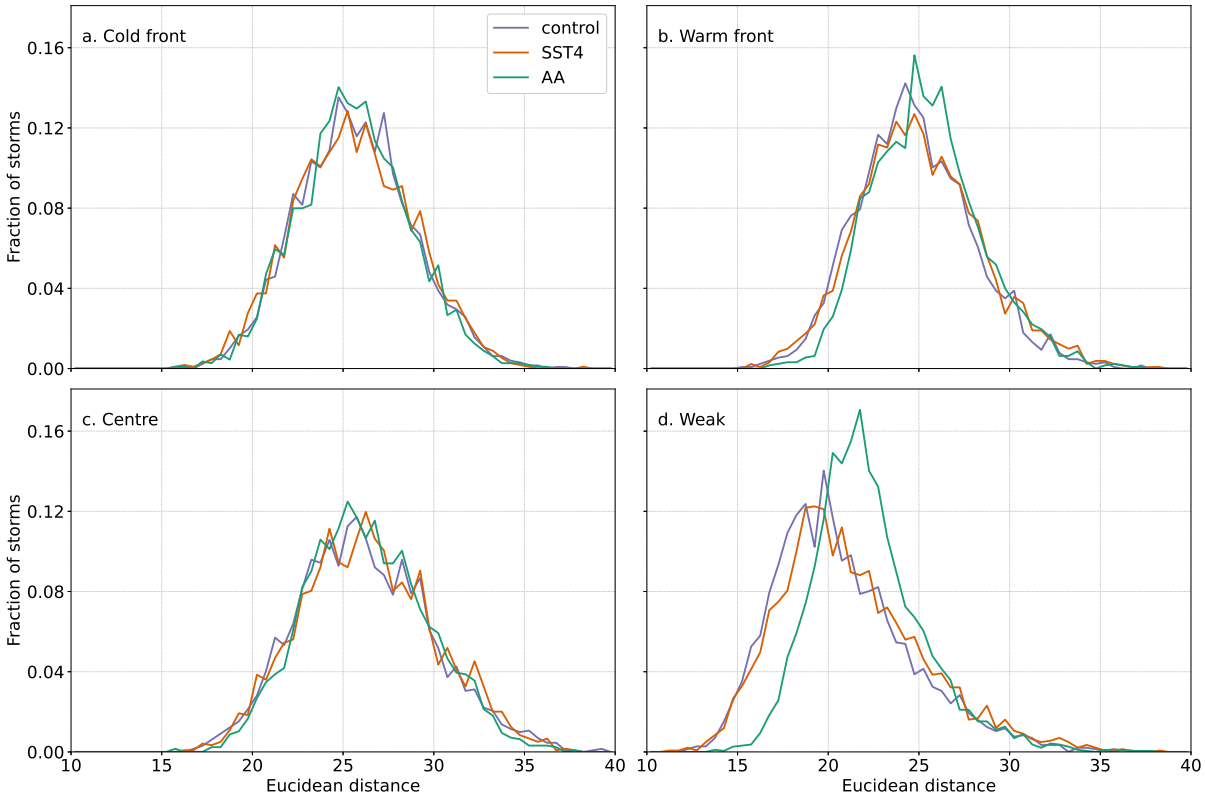

Figure S3: Normalised distributions of the Euclidean distance between each cyclone allocated to a cluster and the centroid of that cluster for the (a) cold front, (b) warm front, (c) centre and (d) weak clusters. The different experiments are shown in different colours.

S3 Separation of clusters and within cluster variability

Once each ETC is allocated to a cluster, we computed the Euclidean distance between each individual ETC and the centroid of the cluster than it was assigned to. The resulting distributions are shown in Figure S3 which allow us to quantify how much variability there is within each cluster and whether the variability within each cluster changes between the three different experiments. For the cold, warm and centre cluster, the amount of variability is very similar in all three experiments. In contrast, for the weak cluster the variability is larger in the AA experiment compared to both the control and SST4 experiments.

In addition, we also computed the Euclidean distance between each individual ETC and the centroid of all other clusters to ascertain how distinct the clusters were. The mean values of the Euclidean distance between all individual ETCs and the centroids of each cluster are shown in Figure S4. The smallest values lie along the diagonal meaning that the individual ETCs are, on average, assigned to the most appropriate cluster. The most difference clusters are the cold front and the weak cluster and this is the case in all three experiments.

S4 Zonal and time mean atmospheric structure

Figure S5 shows the response of the potential temperature gradient and stability in both the SST4 and AA experiments. Uniform warming does not cause any notable changes to the potential temperature gradient at low levels. However, warming causes the troposphere to deepen and the height of the tropopause to increase. This leads to a vertically aligned dipole structure in the potential temperature gradient located near the tropopause with an increase in temperature gradient below the tropopause

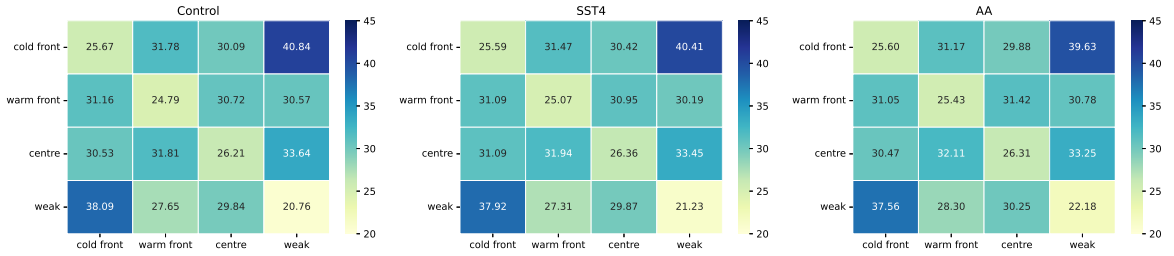

Figure S4: mean Euclidean distance between individual ETCs and the centre of all clusters. Cluster names on the x-axis refer to the cluster centre to which the individual ETCs are compared to whereas cluster names on the y-axis refer to the cluster that the individual ETCs are taken from.

and an decrease above. Uniform warming causes the stability to increase almost everywhere in the troposphere with the most pronouced increase in the tropical upper troposphere. However, increases in stability in the baroclinic zones are also evident and likely act the decrease the intensity of extra-tropical cyclones.

Polar warming causes a localised decrease in the meridional potential temperature gradient which is most pronounced at the surface (minimum value of -0.35 K / 100 km) and between 45° and 57° north and south (Fig. S5c). This potentially acts to weaken extra-tropical cyclones in this region. Polar warming also causes the stability to decreases in the low-to-mid troposphere in the polar regions (Fig. S5d), primarily north and south of 60°, which potentially allows stronger or more ETCs to develop at high latitudes.

S5 The relationship between precipitation and cyclone intensity at different times

Figures S6 and S7 shows the relationship between maximum vorticity and precipitation 24 hours and 0 hours before the time of maximum vorticity. These relationship, and how they differs between the three experiments, is very similar to the relationship maximum vorticity and precipitation 12 hours before the time of maximum vorticity, as shown in Figure 3 of the manuscript. The main differences are that the slopes and correlation coefficients are slightly lower when precipitation 24 hours before the time of maximum intensity is considered compared to precipitation 12 hours before the time of maximum intensity. More notable is that the slopes and correlation coefficient decrease more rapidly between 12 hours before and 0 hours before and as such the relationship between maximum vorticity and precipitation is much weaker when precipitation at the time of maximum vorticity is considered.

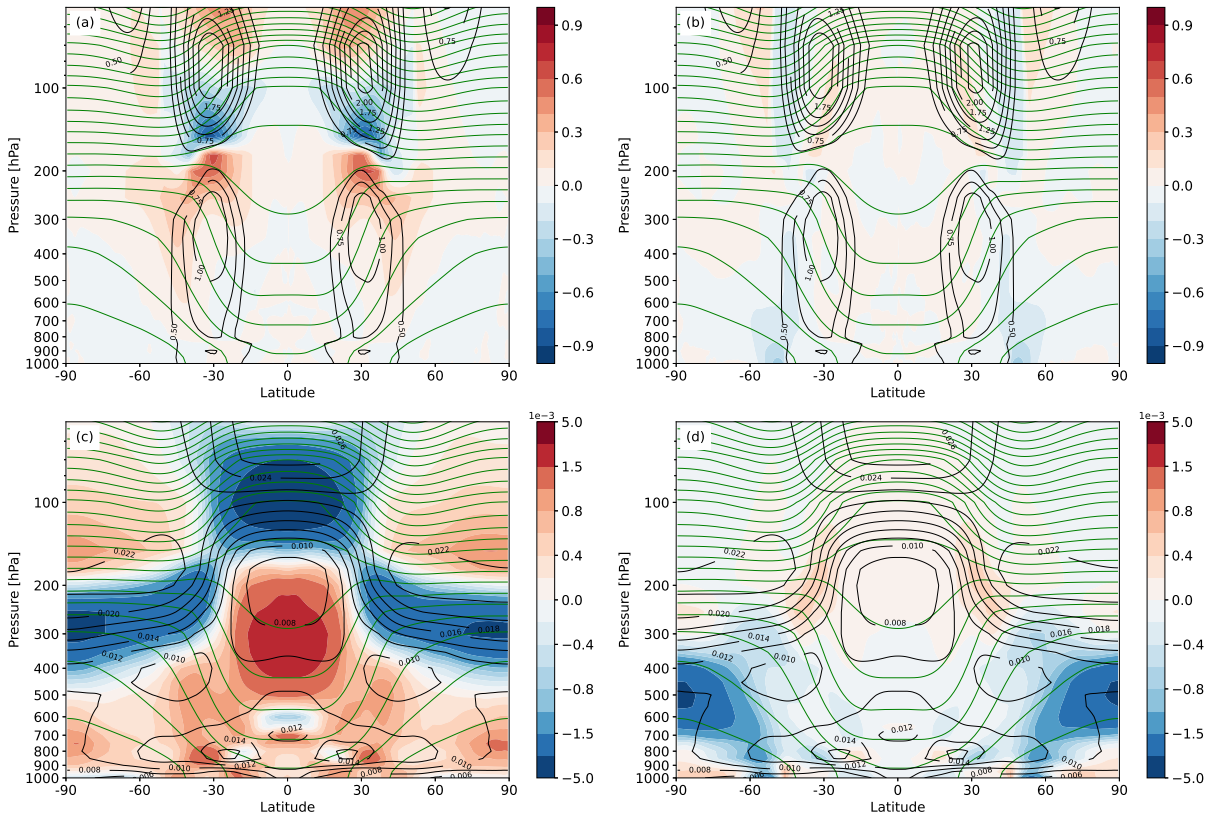

Figure S5: Zonal and time mean fields averaged over 10 years of simulation. (a) Potential temperature (green contours, contour interval 10K) and the absolute meridional potential temperature gradient (black contours, contour interval 0.25 K / 100 km) in the control simulation. Shading shows the difference in the meridional temperature gradient between the control and SST4 simulation (SST4 - control) in K / 100 km. Panel b is the same as a except the shading shows the difference between the control and AA. (c) shows the potential temperature (green contours, contour interval 10K) and the Brunt Väisälä frequency (black contours, contour interval 0.002 s^{-1}) in the control simulation. Shading shows the difference in the Brunt Väisälä frequency between the control and SST4 simulation. Panel (d) is the same as (c) except the difference is between the control and the AA experiment. Note the non-linear colourbar in panels c and d.

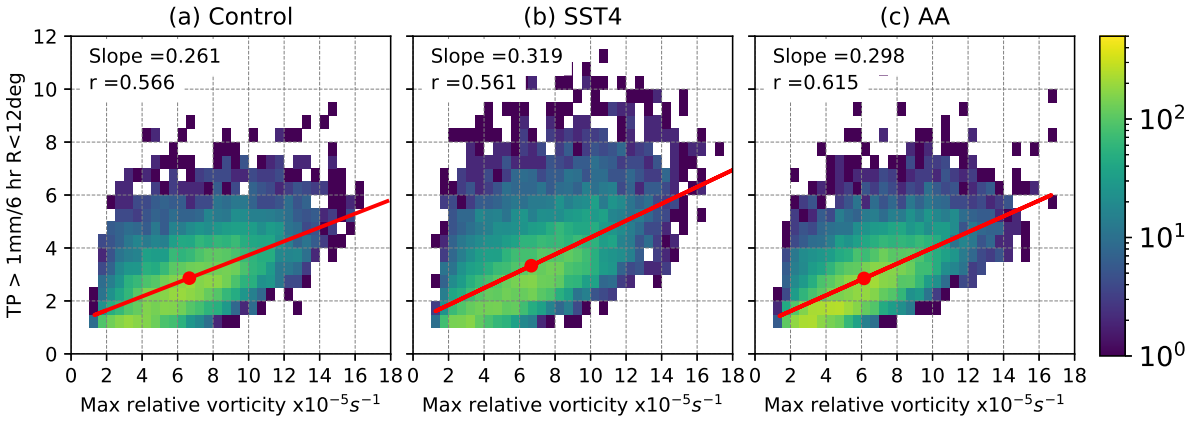

Figure S6: Two-dimensional histograms showing the relation between maximum relative vorticity and ETC-related precipitation 24 hours before the time of maximum relative vorticity. Precipitation is the area average, averaged over all points with a 12 degree radius of the cyclone centre where the rain rate exceeded 1 mm / 6 hr. Only ETCs which exist at -24 hr and have their maximum vorticity north of 30°N are included.

S6 Bootstrapping

Bootstrapping is used to determine if the slope of the regression line between maximum vorticity and ETC precipitation differs between the three experiments. For each experiment, the data was re-sampled with replacement 5000 times using a sample size equal to that of each original data set. For each of the 5000 samples, the slope was computed and the distribution of these, for all three experiments, are shown in Figure S5. A student's t-test shows that the slopes are all statistically significantly different at the 99% level.

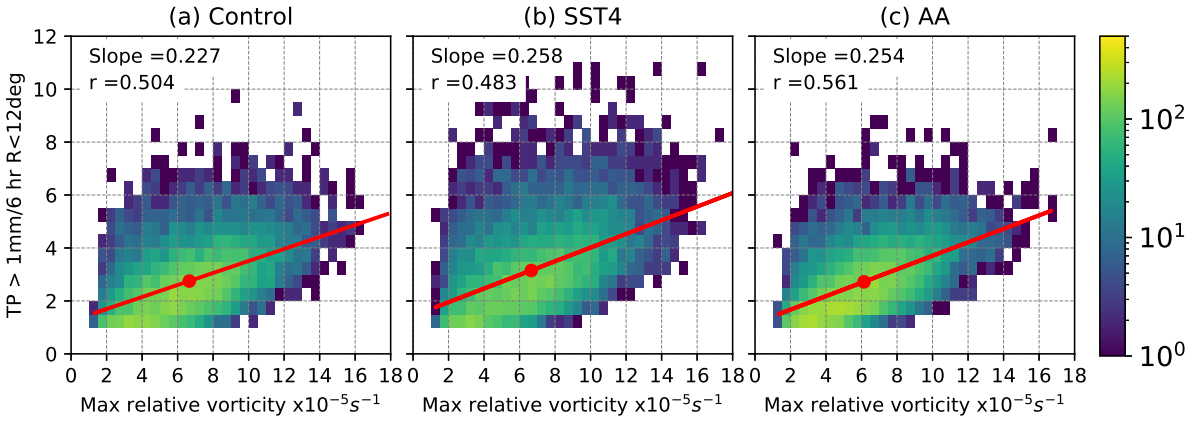

Figure S7: Two-dimensional histograms showing the relation between maximum relative vorticity and ETC-related precipitation at the time of maximum relative vorticity. Precipitation is the area average, averaged over all points with a 12 degree radius of the cyclone centre where the rain rate exceeded 1 mm / 6 hr. Only ETCs which exist at -24 hr and have their maximum vorticity north of 30°N are included.

S7 Time evolution of clusters in all experiments

In the paper, we focused on the the structure of the ETC clusters 12 hours before the time of maximum vorticity. For completeness, in Figures S6 - S8 we show the time evolution of each cluster in each experiment from 72 hours before the time of maximum vorticity to the time of maximum vorticity. The main points are:

1. In all three experiments, there is little different between the 4 clusters 72 hours before the time of maximum vorticity when the precipitation pattern is considered.

2. In all experiments, the weak ETC has slightly heavier precipitation associated with it at 72 and 48 hours before the time of maximum vorticity compared to 24, 12 and 0 hours before the time of maximum vorticity.

3. For the cold front, warm front and centre ETC, there are only small differences in the precipitation pattern between 24, 12 and 0 hours before the time of maximum vorticity. However, for all of these ETCs, the precipitation pattern does rotate slightly cyclonically around the ETC centre as the ETC approaches its maximum vorticity.

4. In all experiments, the cold front and centre ETC have their heaviest precipitation 12 hours before the time of maximum vorticity. In contrast, the warm front ETC does not see a notable increase in the maximum precipitation rate between 24 and 12 hours before the time of maximum vorticity.

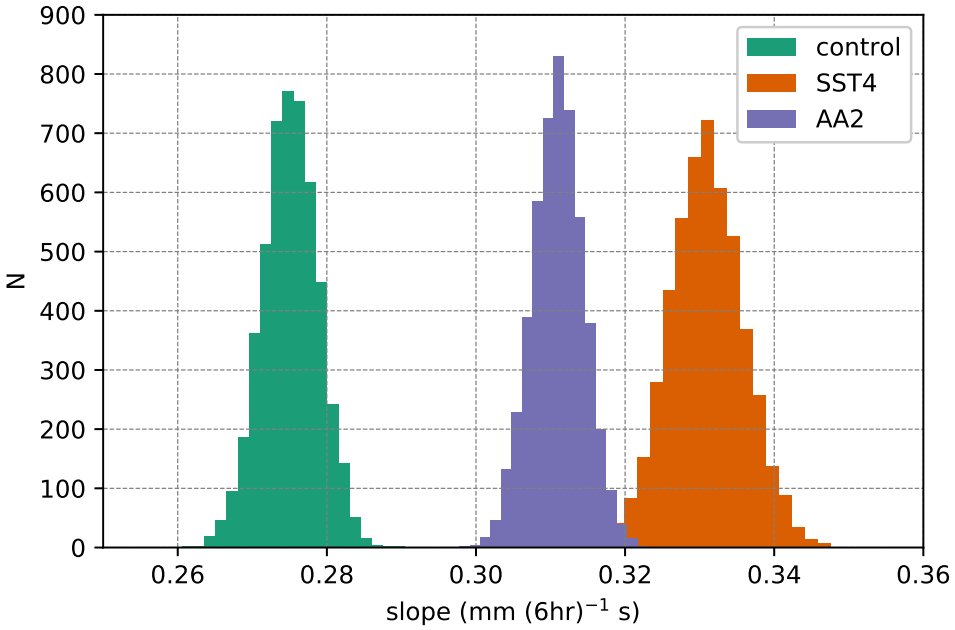

Figure S8: Distributions of the slopes between maximum vorticity and precipitation 12 hours before the time of maximum vorticity obtained from bootstrapping.

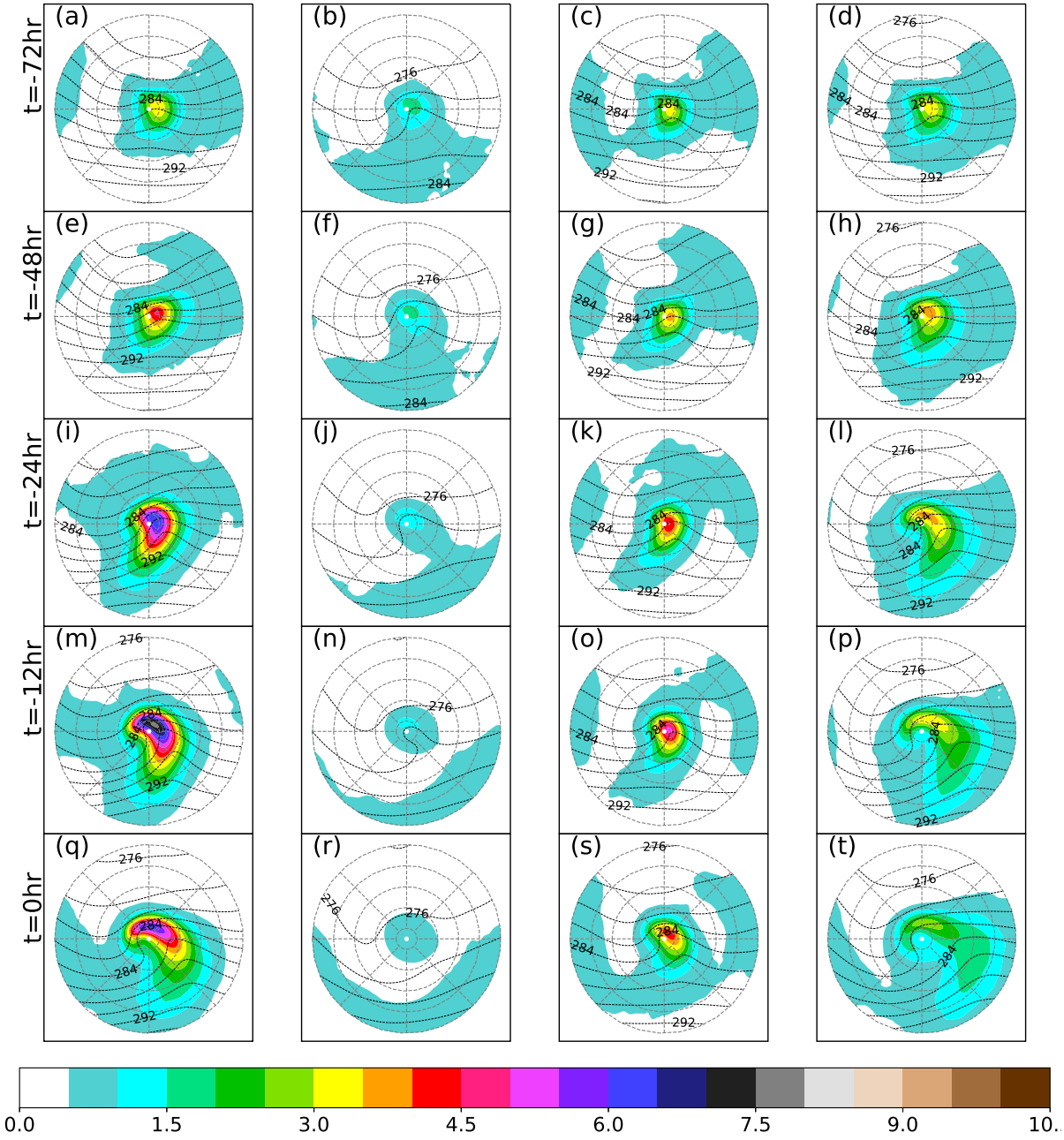

Figure S9: Cluster mean total precipitation (mm / 6 hr) and 850-hPa potential temperature (contours every 1 K) at different offset times relative to the time of maximum vorticity for the control simulation. Each column shows the evolution of a different cluster.

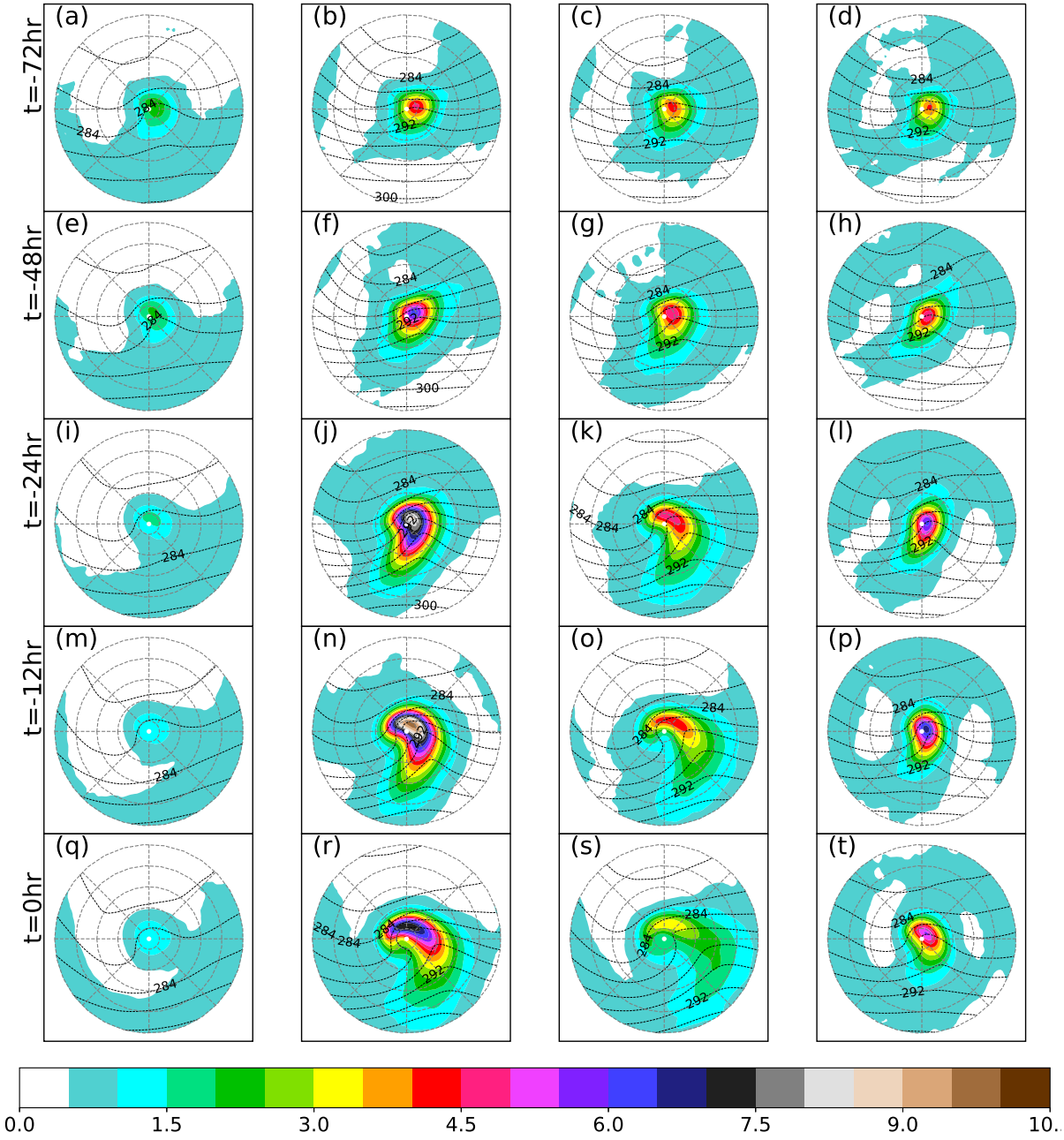

Figure S10: Cluster mean total precipitation (mm / 6 hr) and 850-hPa potential temperature (contours every 1 K) at different offset times relative to the time of maximum vorticity for the SST4 simulation. Each column shows the evolution of a different cluster.

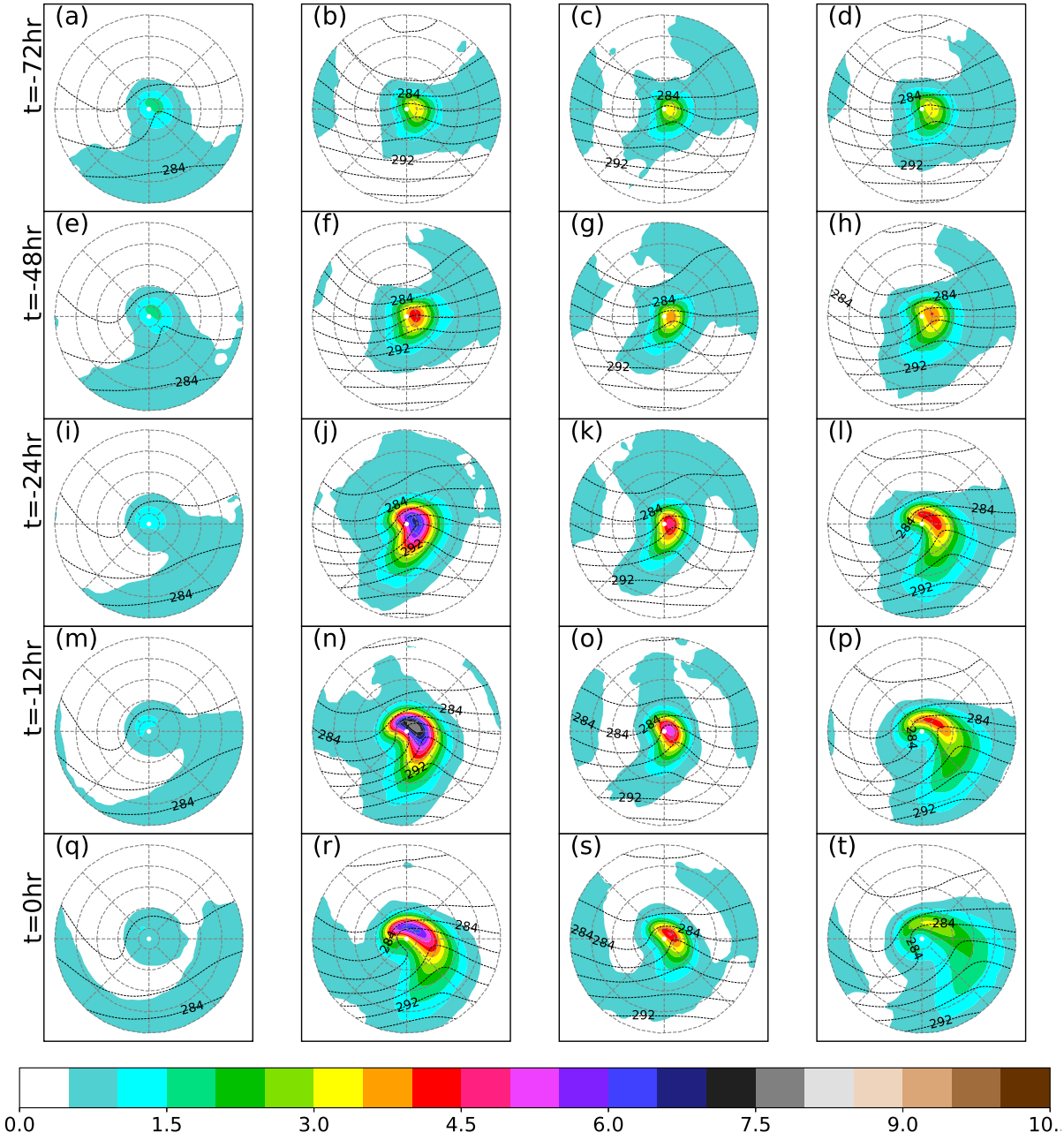

Figure S11: Cluster mean precipitation (mm / 6 hr) and 850-hPa potential temperature (contours every 1 K) at different offset times relative to the time of maximum vorticity for the AA simulation. Each column shows the evolution of a different cluster.